

Boosting 3-acetamido-5-acetyl furan production from *N*-acetyl-D-glucosamine in γ -valerolactone by a dissolution-dehydration effect

Xinlei Ji ^a, Jia Kou ^a, Gökulp Gözaydin ^b, Xi Chen ^{a,*}

^a China-UK Low Carbon College, Shanghai Jiao Tong University, 3 Yinlian Rd, 201306 Shanghai, China

^b Department of Chemical and Biomolecular Engineering, National University of Singapore, 117585, Singapore



ARTICLE INFO

Keywords:

Biomass refinery
Chitin
Dehydration
Green solvent
Organonitrogen

ABSTRACT

Chitin biorefinery offers a unique opportunity to sustainably produce highly-valued organonitrogen compounds such as the versatile pharmaceutical precursor 3-acetamido-5-acetyl furan (3A5AF), bypassing the Haber process and mitigating the consumption of fossil feedstocks. However, the reported protocols engaged large quantities of toxic organic solvents and required harsh conditions. In this work, a highly efficient catalytic system has been developed in the nontoxic, biobased γ -valerolactone (GVL) solvent under relatively mild conditions. 3A5AF was selectively obtained with an unprecedented yield of 75.3% at 140 °C for 2 h by adding NH₄SCN and HCl. The high yielding was exclusively promoted by a dissolution-dehydration effect. Based on the UPLC-TOF-MS and NMR analyses, the presence of NH₄SCN has induced a very rapid NAG conversion possibly by coordinating with the acetamido group and the hydroxyl groups, and the 3A5AF product was obtained in a subsequent dehydration pathway from NAG with the Chromogen I and Chromogen III as the intermediates.

1. Introduction

Global warming and climate change have become one of the greatest environmental issues of the century [1–6]. Seeking alternative renewable resources to substitute the fossil feedstocks to produce fuel, chemicals and materials are paramount to mitigate climate change and eventually achieve the sustainable development of the society [7–12]. Biomass is the largest renewable carbon source in the world which can be utilized as an abundant, inexpensive and widely-available raw material to generate energy and chemicals [13–20]. Chitin is an amino-biopolymer consisting of mainly the *N*-acetyl-D-glucosamine (NAG) repeating units from oceanic wastes with an annual production of ~100 billion tons [21]. With all the necessary elements in the natural structure, chitin is a platform feedstock to produce a series of highly-valued organonitrogen compounds bypassing the energy-intensive Haber process for nitrogen fixation [22–26]. The ammonia synthesis process alone accounts for approximately 1–2% of the global carbon emission [27,28]. Hence, enlarging the biorefinery boundary from chitin towards organonitrogen compounds will not only diversify the biobased product stream and elevate the economic competitiveness, but also contribute to waste management and global

warming mitigation [29]. Among the chitin-derived organonitrogen chemicals, 3-acetamido-5-acetyl furan (3A5AF) is a versatile building block chemical (an analog to 5-hydroxymethylfurfural (5-HMF) in cellulose conversion [30–32]) with pronounced market prospects, which can be upgraded into various amino-sugars, *N*-heterocycles, pharmaceuticals and bioactive molecules [33]. For instance, 3A5AF is the constituting moiety of the anticancer alkaloids (proximicins), and the synthesis route from chitin via 3A5AF for the alkaloid has been proved notably more sustainable and efficient with a shortened pathway compared to the non-renewable fossil-based route [34–36].

However, the current synthesis protocols using toxic and expensive solvents under high temperatures remarkably hindered the practical applications. Pioneering studies on NAG and chitin conversion into 3A5AF were demonstrated by Kerton [37,38] and Yan's group [39,40] using boric acid in [BMIm]Cl ionic liquids (ILs) or *N,N*-dimethylacetamide (DMA)/*N*-Methyl-2-pyrrolidone (NMP) solvents at 180–220 °C. Zang's group has reported various ILs (such as [Gly]Cl) as the catalysts for NAG dehydration into 3A5AF at 170–190 °C with 42–69% yields in DMA or NMP [41,42]. Zhang's group employed ammonium salts as catalysts for the reaction in DMA or *N,N*-dimethylformamide (DMF) at about 180 °C to produce 3A5AF with 56.7% yield [43]. Fukuoka's group

* Corresponding author.

E-mail address: chenxi-lcc@sjtu.edu.cn (X. Chen).

has brought down the reaction temperature to 120 °C using AlCl_3 catalyst but the solvent was still DMF and the 3A5AF yield was relatively low of ~30% [44]. The use of safer solvents is one of the twelve principles for green chemistry to considerably reduce the environmental impact, capital costs, and personnel safety risks of a chemical reaction [45]. Unfortunately, DMA, DMF, etc. are very toxic and hazardous which may cause liver damage, interfere with the human reproductive system, etc. The $[\text{BMIm}]Cl$ ILs are expensive, extremely sensitive to moisture and major concerns have been raised on their potential toxicity to humans and environments. Hence, selective and efficient production of 3A5AF from chitin biomass in a green solvent under relatively mild conditions is highly desirable and beneficial, which has not yet been achieved.

Efforts have been constantly made to find alternative green solvents to the toxic DMF, DMA, NMP solvents for catalytic biomass conversion [46]. γ -Valerolactone (GVL) is a naturally-existed, nontoxic and biomass-derived compound which could serve as a stable polar aprotic green solvent [47–52]. GVL has been reported as the solvent for cellulose hydrolysis and glucose dehydration [53–57]. For chitin biomass conversion, the chitin or chitin monomers are insoluble in GVL under ambient temperature and thus harsh conditions (e.g. 180–200 °C) are often demanded to enable efficient mass transfer and chemical transformation. In this work, a green, facile and efficient method was developed for NAG dehydration into 3A5AF in GVL. Under optimal reaction conditions, the highest 3A5AF yield of 75.3% could be achieved at a lower temperature range of 130–150 °C with the reaction times of 45–180 min by the combinational use of NH_4SCN and HCl as the catalyst. The presence of NH_4SCN has not only facilitated the dissolution of NAG in GVL (~100% solubility compared to only ~14% without NH_4SCN addition) but also enabled an extremely fast NAG conversion and dehydration based on the solubility tests and NMR analyses. A plausible reaction pathway was identified and proposed that the NH_4SCN probably coordinated with NAG on multiple sites (the acetamido and -OH groups) to promote NAG dehydration first to Chromogen I which was subsequently converted to Chromogen III, and eventually the dehydration of Chromogen III resulted in the 3A5AF production.

2. Experimental Sections

2.1. Materials

Chitin powder (92%, degree of acetylation (DA) was 90.7%), D-glucosamine hydrochloride (RG, 99%), D-Fructose (RG, 99%), and dimethyl sulfoxide- d_6 (DMSO- d_6 , 99.9 atom % D) was purchased from Sigma-Aldrich Co., Ltd. *N*-Acetyl-D-glucosamine (NAG, ≥ 98%) was purchased from TCI (Shanghai) Chemical Industry Development Co., Ltd. Acetonitrile (≥ 99.9%), activated carbon, D-Glucose (AR), calcium chloride (CaCl_2 , anhydrous, 97%), lithium chloride (LiCl , anhydrous, 98%), formic acid (HCOOH , ≥ 98%), lithium bromide (LiBr , 99%), ammonium chloride (NH_4Cl , 99.5%), manganese chloride (MnCl_2 , 98%), aluminum chloride (AlCl_3 , 99%), ammonium bromide (NH_4Br , 99.0%), ammonium bisulfate (NH_4HSO_4 , 98%) and N,N-dimethylformamide (DMF, ≥ 99.9%) were purchased from Aladdin Reagent Company. Sodium chloride (NaCl , 99.5%), potassium thiocyanate (KSCN , ≥ 98.5%), copper (II) chloride dihydrate ($\text{CuCl}_2 \cdot 2 \text{H}_2\text{O}$, ≥ 99.0%) and thiourea ($\text{CH}_4\text{N}_2\text{S}$, ≥ 99.0%) were purchased from General Reagent. Magnesium chloride (MgCl_2 , 99%) was purchased from Leyan. Ethyl acetate (EtOAc , 99%), γ -valerolactone (GVL, 98%), propylene carbonate (PC, 99%), zinc chloride (ZnCl_2 , 98%), ferric chloride hexahydrate ($\text{FeCl}_3 \cdot 6\text{H}_2\text{O}$, 99%), iron tribromide (FeBr_3 , 98%), ferrous chloride tetrahydrate ($\text{FeCl}_2 \cdot 4\text{H}_2\text{O}$, 99.95%), Sodium bromide (NaBr , 99%), zinc chloride (ZnCl_2 , 98%), phosphoric acid (H_3PO_4 , ≥ 85 wt% in H_2O , ≥ 99.99% metals basis) and DMSO (≥ 99.8%) were purchased from Shanghai Machlin Biochemical Co., Ltd. DMA (99%) was purchased from Source Leaf Organisms. Acetic acid (CH_3COOH , ≥ 99.5%), magnesium bromide (MgBr_2 , 99%, metal basis), tin (IV) chloride

dihydrate ($\text{SnCl}_2 \cdot 2\text{H}_2\text{O}$, 99.5%+), chromium chloride (III) (CrCl_3 , 98%+), barium chloride dihydrate ($\text{BaCl}_2 \cdot 2\text{H}_2\text{O}$, 99%+), 5-HMF, and zinc acetate ($\text{Zn}(\text{CH}_3\text{COO})_2$, anhydrous, 99.5%+) were purchased from Adamas Reagent Co., Ltd. D_2O (99.9% D, for NMR) was purchased from Energy Chemical. Ammonium thiocyanate (NH_4SCN , ≥ 98.5%), sodium thiocyanate (NaSCN , ≥ 98.5%), ammonium sulfate (NH_4SO_4 , ≥ 99.0%), ammonium dihydrogen phosphate ($\text{NH}_4\text{H}_2\text{PO}_4$, ≥ 99.0%), zinc bromide (ZnBr_2 , ≥ 98.5%), boric acid (BA, ≥ 99.5%), D-xylose (BR), lactic acid, ethanol (Anhydrous, ≥ 99.5%), hydrochloric acid (HCl, 38%) and sulfuric acid (H_2SO_4 , 98%) were purchased from Sinopharm Chemical Reagent Co., Ltd. Nickel (II) chloride hexahydrate ($\text{NiCl}_2 \cdot 6\text{H}_2\text{O}$, 99%) was purchased from Innochem (Beijing) Technology Co., Ltd. Ultrapure water with conductivity less than 18.25 $\text{M}\Omega/\text{cm}$ was used in this work. All chemicals were used without further purification.

2.2. Conversion of NAG

The dehydration reactions of NAG were performed in a parallel reactor using thick-wall glass tubes. Typically, 100–500 mol% catalyst based on the moles of NAG was weighed and placed into a thick-wall glass tube, following that 4 mL solvent (GVL, PC, DMA, DMF or DMSO) was added. After preheating the solution with a stirrer bar at the controlled temperature for about 5 min, 50–250 mg NAG and 25–250 mol% additive (or without additive) were loaded. Then the tube was sealed by a PTFE cap and placed into the parallel reactor at the controlled temperature for specified reaction time. After the reaction, the reaction mixture was cooled down to room temperature and then filtered by a PTFE syringe filter with a 0.2 μm pore size before analyzing by high-performance liquid chromatography (HPLC).

2.3. Conversion of chitin

Three pretreatment methods have been used for the direct conversion of chitin. First, ball milling: 800 mg chitin (3.62 mmol based on a number of NAG units) was loaded into the planetary ball mill grinder (XQM) at 500 rpm by using zirconia balls (diameter 5 mm, 100 g) with 3 h total mill time (10 min mill and 10 min rest as a cycle) in a zirconia pot (125 mL volume). The product denoted as BM chitin. Second, aging method: 1.66 g of chitin (8.18 mmol based on a number of NAG units) was dispersed in 5 mL of diethyl ether containing 54.3 μL of H_2SO_4 (1.02 mmol) with stirring. At room temperature in summer, diethyl ether completely evaporated after several minutes of stirring. Chitin samples containing H_2SO_4 were aged at 40 °C for 48 h in an oven, the product denoted as aged chitin. Third, acid ball milling: 800 mg chitin (3.62 mmol based on a number of NAG units) and 53.0 μL of H_2SO_4 (0.90 mmol) were loaded together into the planetary ball mill grinder (XQM). The other parameters used in acid ball milling process were identical to those employed for BM chitin. The product denoted as acid-BM chitin.

The dehydration reactions of chitin were also performed in a parallel reactor equipped with thick-walled glass tubes in a similar manner with NAG. In a typical reaction, a certain mass of NH_4SCN based on the moles of monomer unit of chitin was weighed and placed in a thick-walled glass tube, followed by the addition of total 4 mL of GVL or GVL with co-solvent (MSHs). After preheating the solution with a stirrer bar at the controlled temperature for about 5 min, substrate (untreated chitin or pretreated chitin samples) and HCl were added. Then the tube was sealed by a PTFE cap and placed into the parallel reactor at the controlled temperature for desired reaction time. After the reaction, the reaction mixture was cooled down to room temperature and then filtered by a PTFE syringe filter with a 0.2 μm pore size before analyzing by HPLC.

2.4. Solubility tests

The solubility of NAG in GVL in the absence or presence of catalyst was tested. The solubility values were recorded after heating for a while

(2–3 min) because NAG was almost insoluble in GVL at room temperature with or without a catalyst. Typically, 200 mol% catalyst (the amount of NH_4SCN has been varied from 100 mol% to 500 mol%) based on the moles of NAG was weighed and placed into a thick-wall glass tube, following that 4 mL GVL was added. After preheating the solution with a stirrer bar at 140 °C for about 5 min, 100 mg NAG was loaded and maintained at 140 °C for 2–3 min. Then the remaining solid was washed with ethanol and centrifuged at 9000 rpm for 15 min for three times, and dried for 24 h at 70 °C in an oven. The solubility of NAG is calculated using the equation as shown below:

$$\text{NAG solubility (wt\%)} = (\text{initial NAG (mg)} - \text{remaining solids(mg)}) / \text{initial NAG (mg)} \times 100\%.$$

2.5. Product identification

HPLC used for quantitative analysis was performed on SHIMADZU LC-20AT system equipped with photodiode array detector (PAD) and refractive index detector (RID) by using Shim-pack GIST C18 column (4.6 I.D. × 250 mm, 5 μm). The temperature of the column was maintained at 35 °C. The mobile phase was 83% water and 17% acetonitrile with a flow rate of 0.6 mL/min and run for 18 min. The UV-vis detector was set at 230 nm to analyze the 3A5AF product. The preparation of 3A5AF standard sample was performed following a literature method [44] and the purity was confirmed by nuclear magnetic resonance (NMR) spectroscopy (Fig. S1). The 3A5AF concentration was quantified by using a calibration curve of 3A5AF plotted by the standard sample (Fig. S2), and the yield of 3A5AF was calculated using the following equation:

$$\text{3A5AF yield \%} = (\text{moles of 3A5AF}) / (\text{moles of monomer unit}) \times 100\%$$

The detection of NAG and other possible dehydration products were conducted on HPLC using an Agilent Hi-Plex H column (7.7 I.D. × 300 mm, 8 μm) at 60 °C oven temperature. The mobile phase was 5 mM H_2SO_4 aqueous solution with a flow rate of 0.6 mL/min. The reaction intermediates were qualitatively analyzed by UHPLC/supercritical fluid chromatography-quadrupole time-of-flight mass spectrometry (UPLC-TOF-MS) using an Acquity 2D-UPLC/Acquity UPC2/Xevo G2-XS QTOF from Waters. The NAG and NH_4SCN mixture aqueous solution (NAG: $\text{NH}_4\text{SCN} = 1:4$) was directly injected into TOF-MS.

2.6. Recyclability tests and product separation

The recyclability tests have been conducted by using two methods. The first one is direct reaction and recycling: after the reaction under the optimized conditions, the reaction solution was filtered using a 0.2 μm pore size PTFE membrane filter. Fresh NAG and GVL (minor loss during filtration) was supplied into the solution for the subsequent runs. The accumulated 3A5AF yield was calculated and the product yield in each run was obtained by subtracting the values of the current run with the previous run. For the second method, an absorption treatment step was added. The reaction solution was stirred with activated carbon (100 mg) for 30 min and then filtered. Besides replenishing NAG and GVL, a small amount of the catalysts have been supplemented because the activated carbon would also remove some of the catalysts [58]. For 3A5AF separation, equal volume of water (30 mL water) was added to the filtered reaction solution, followed by extraction using 15 mL EtOAc. The extraction was conducted for four times and the extractive phase was combined. The organic phase was obtained by centrifuging the mixture at 7000 rpm for 10 min. The extractive phase was then evaporated on a rotary evaporator at elevated temperature (gradually heated to 85 °C) under vacuum to remove the solvent. The purified solids were weighed and analyzed on HPLC and only the peak of 3A5AF appeared on the spectrum.

2.7. Kinetic study and NMR analyses

The initial rates were fitted to first-order rate plots based on the 3A5AF concentration at low temperatures (85–100 °C) when the 3A5AF yield was lower than 7%. The Arrhenius plot of \ln (initial rate) vs. $1/T$ was generated and used to calculate the apparent activation energy. Liquid ^{13}C NMR and ^1H NMR spectroscopy analyses were performed on a Bruker AVANCE NEO 700 MHz instrument. NMR analysis of the reaction samples with different reaction time and temperature were carried out to identify the interaction in the reaction system. The samples of 100 mg NAG with the addition of 400 mol% NH_4SCN in GVL were prepared. In this study, reaction samples with reaction time of 2 min, 5 min, 15 min, 30 min, 45 min and 60 min at 130 °C and with reaction temperature of 90 °C, 100 °C, 110 °C for 2 min were selected for analysis. Besides, three samples were studied in $\text{DMSO}-d_6$ solvent, which were pure NAG, NAG together with 400 mol% NH_4SCN , NAG with 400 mol% NH_4SCN heating at 80 °C for 5 min

3. Results and discussion

3.1. Catalyst effect

A series of catalysts were used (> 30 different species) including metal halides, ammonium salts, acids, etc. to testify the possibilities of converting NAG into 3A5AF in GVL at 140 °C for 30 min (Fig. 1a). Most of the selected catalysts were previously proved active for biomass dehydrations [59–61]. Under employed conditions, the 3A5AF product was probed in the presence of the following catalysts in descending yields: NH_4SCN (26.2%) > MgCl_2 (15.6%) > LiBr (10.7%) > MgBr_2 (8.9%) > HCl (6.8%) > LiCl (2.0%). NH_4SCN has displayed the best performance to promote 3A5AF formation in GVL. Although boric acid and AlCl_3 have been reported effective for NAG dehydration in DMF solvent [37–40,44], these catalysts were almost inactive in GVL with negligible 3A5AF generation, which possibly indicates a solvent-mediated effect on the catalytic performance. Aside from NH_4SCN , other ammonium salts and thiocyanates (with different cations or anions) have been evaluated. Nevertheless, 3A5AF product was obtained in very low yields of 4.0% and 2.0% by adding NH_4Cl and NH_4Br , and barely detected when using other ammonium or thiocyanate salts. Hence, the promotional effect of NH_4SCN is relatively unique, of which the cation and anion probably played synergistic roles on 3A5AF formation.

The thiocyanate salts have been previously engaged for cellulose dissolution and pretreatment. For instance, the $\text{Ca}(\text{NCS})_2$ molten salt hydrates (MSHs) could deconstruct the extensive hydrogen bond networks among cellulose polymer chains and facilitate its dissolution [62]. In addition, the $\text{NH}_4\text{SCN}-\text{NH}_3$ solvent system has been reported to pretreat lignocellulosic biomass at ambient environment [63]. The NH_4SCN functioned as both hydrogen bond donor and acceptor to interact with the -OH groups on cellulose. Note that NAG was not soluble in GVL at either room temperature or elevated temperature, we conjecture that the small amount of NH_4SCN in GVL may stimulate NAG dissolution and the solvation effect is crucial for improved mass transfer and catalysis [64]. For comparison (Fig. 1b), the images of solutions without a catalyst and with different catalysts (NH_4SCN , MgCl_2 , LiBr , KSCN and NH_4Br) were recorded at the examined reaction temperature of 140 °C (heating for about 2–3 min). From the images and the solubility tests, NAG was seldomly dissolved (the solubility of about 13.8%) with a rapid heating at 140 °C in the absence of a catalyst. The addition of NH_4Br and KSCN has caused volume expansion to different extents, but the changes were inconspicuous in terms of solubility and color. The NAG solubility in the presence of NH_4Br and KSCN were determined to be 14.8% and 14.3%. The addition of LiBr has exceptionally promoted the dissolution of NAG (determined as 100% in solubility tests) and a transparent solution was obtained with negligible solid residues. In contrast, the MgCl_2 addition did not obviously promote dissolution (16.0% solubility) but

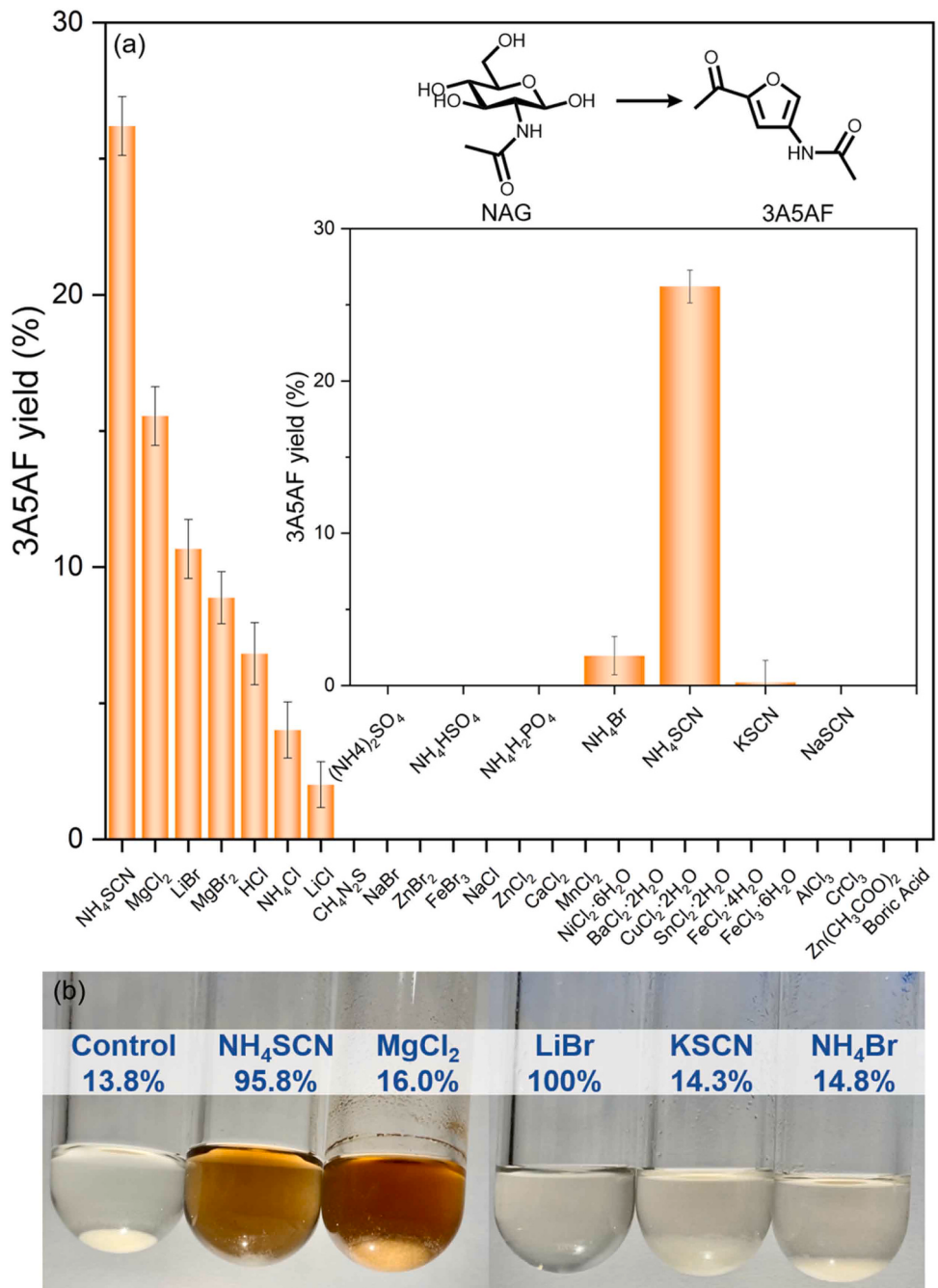


Fig. 1. (a) The effect of different catalysts on the NAG conversion to 3A5AF. Reaction conditions: NAG (100 mg), catalyst (200 mol%) in GVL (4 mL) at 140 °C for 30 min (b) The solubility tests of NAG in GVL. Solubility test conditions: NAG (100 mg), catalyst (200 mol%) in GVL (4 mL) at 140 °C for 2–3 min. The values on Fig. 1b denote the solubility of NAG in corresponding solutions.

the solution color has evidently altered from transparent to brownish. The color change denotes the occurrence of chemical reactions and infers the relative strong ability of MgCl_2 to catalyze the reaction within a very short period. In the presence of NH_4SCN , the solubility of NAG has been remarkably enhanced to 95.8% and a similar color change of the solution from transparent to brownish was observed at the same time. The solubility tests of NAG in GVL by adding different amounts of NH_4SCN have been recorded (Fig. S3). The increase in NH_4SCN amount is beneficial for NAG dissolution and 100% solubility was achieved by adding 400 mol% NH_4SCN . Besides, the color change from yellow to brownish also indicates that more NH_4SCN possibly favored the dehydration reaction. In addition, the change in pH value and ionic strength might also played positive roles on NAG dehydration. As shown in

Table S1, the pH decreased from 3.77 to 3.31 with the increase of NH_4SCN addition from 100 mol% to 500 mol%, and the acidic environment could be favorable for dehydration. Previous literatures [65–67] have demonstrated that varied ionic strength could affect the dissolution properties. Hence, super-stoichiometric NH_4SCN is necessary to efficiently facilitate NAG dissolution and dehydration to produce 3A5AF. In the catalyst screening, the three catalysts of LiBr , MgCl_2 and NH_4SCN were able to produce 3A5AF and the NH_4SCN was much superior to the rest two. Based on the experimental results and the observations, both the dissolution and catalytic dehydration ability of the catalyst are critical for NAG dehydration. The NH_4SCN could concurrently enable effective NAG dissolution and efficient catalytic dehydration, and this dissolution-dehydration synergy has considerably

boosted the 3A5AF yield in GVL.

3.2. Solvent effect

To grasp the solvent effect, the reactions have been examined in five different solvents (GVL, PC, DMF, DMA, DMSO) in the presence of the NH₄SCN catalyst (Fig. 2a). Complete conversion of NAG was observed for all the solvents under employed reaction conditions. PC is also regarded as a green solvent because of its low toxicity and good biodegradability which can be synthesized using CO₂ as a raw material [68,69]. The 3A5AF yield is encouraging in PC solvent of 21.8%, slightly lower than that in GVL. On the contrary, the 3A5AF yield was below 5% in DMF, DMA and DMSO which are the commonly-used solvents in previous literatures for NAG dehydration [40–42,44]. Although these conventional solvents are more capable of dissolving NAG (soluble at room temperature), the dehydration performances were much inferior. Based on previous studies, it is deduced that these conventional solvents could only promote NAG dehydration at a higher temperature window (> 180 °C) [70–72]. With the addition of NH₄SCN, the solvation environment for NAG has been much improved to tackle the dissolution problem in GVL, resulting in efficient NAG dehydration under milder temperatures. The apparent activation energy for 3A5AF production was investigated and calculated in GVL to be 102.3 kJ/mol (Fig. 2b), which was comparable to those of glucose dehydration in GVL [73,74]. According to previous literatures [40,72,75], the NAG conversion into 3A5AF often involves the pyranose ring opening, the furan ring formation and the subsequent dehydration steps. The shift of pyranose ring to furan ring is usually considered as the rate-determining step. It is likely that the NH₄SCN would better promote these key steps than the other solvents under employed conditions. As a result, the GVL solvent is not only more sustainable and environmentally benign, but also facilitate the NAG dehydration at a lower temperature with enhanced performance by deploying a suitable catalyst.

3.3. Additive screening and reaction optimizations

To increase the product yield, the combination of a second additive mainly Brønsted and Lewis acids to promote dehydration with the NH₄SCN catalyst was examined (Fig. 3a). Mineral acids such as HCl and H₂SO₄ were favorable for NAG dehydration to incline the 3A5AF yield. On the contrary, the other employed Brønsted and Lewis acid additives (such as HCOOH, CaCl₂, etc.) showed adverse effects with decreased 3A5AF yields. Among them, HCl is the most effective additive to increase the 3A5AF yield from 26.2% to 37.2%. Next, the NH₄SCN dosage was varied from 100 mol% to 500 mol% (Fig. 3b). With increased

dosage to 400 mol%, the 3A5AF yield constantly climbed from 4.9% to 70.2%, suggesting that the dehydration has been facilitated with more NH₄SCN addition. Nonetheless, the 3A5AF yield started to drop with 500 mol% NH₄SCN addition and therefore overdosage of the catalyst was not beneficial. The amount of HCl addition was afterwards investigated with a broad range of 25–250 mol% (Fig. 3c). The optimized HCl amount was 100 mol% producing 3A5AF in 70.2% yield. After this point, the excessive HCl would suppress the yield of 3A5AF. The NAG concentration was varied from 12.5 mg/mL to 62.5 mg/mL (Fig. 3d). Comparable yields of dehydrated products were detected for 12.5 mg/mL and 25 mg/mL feedstock solution. A slight and steady decrease in 3A5AF yield was observed with further increase in substrate concentration. Nonetheless, the 3A5AF yield could maintained at satisfactory yields of 57.0% and 46.3% with relatively concentrated feedstock solutions of 37.5 mg/mL and 50 mg/mL, which demonstrated the potentials in practical applications. Lastly, the influence of water has been analyzed for the reaction system (Fig. 3e). Water is detrimental for chitin dehydration in NMP as previously reported that the 3A5AF yield dropped to almost zero in the presence of > 100 μL water (about 2.5% water content) [40]. In the studied GVL system, the water addition also caused the product yield to decline whereas a satisfactory 3A5AF yield of 48.1% could be maintained in the presence of 150 μL water (about 5% water content), which infers the higher resistance of the developed system using GVL compared to the previous conventional solvent system. This is beneficial in realistic sceneries for large-scale application to be robust against moisture variation and water absorption from the air.

The evolution of 3A5AF product under different temperatures (from 120 °C to 150 °C) with the reaction time from 15 min to 180 min has been monitored (Fig. 4). The two parameters of temperature and time are influential on dehydration and mutually correlated. At lower temperatures of 120 °C and 130 °C, the 3A5AF yield gradually inclined with increased reaction time. At 140 °C, a volcano-shape curve was observed for 3A5AF yield and the peak value of 75.3% occurred at the reaction time of 120 min. At 150 °C, the highest 3A5AF yield was obtained within 45 min and the yield started to constantly decrease afterwards. Besides, 3A5AF was formed much faster at 140 °C and 150 °C with the yields of 54.4% and 67.7% at a reaction time of merely 15 min. According to the results, the reaction kinetics have been considerably accelerated at beyond 140 °C, nevertheless, sharp decrease in 3A5AF was recorded at 150 °C after 45 min possibly due to decomposition or the formation of humins. Overall, an unprecedent 3A5AF yield of > 70% could be achieved in the established reaction system at the relatively mild temperature range of 130–150 °C with prolonged time of 180 min or shortened time of 45 min. To obtain an isolated product yield, the 3A5AF product was purified and separated from the reaction system by

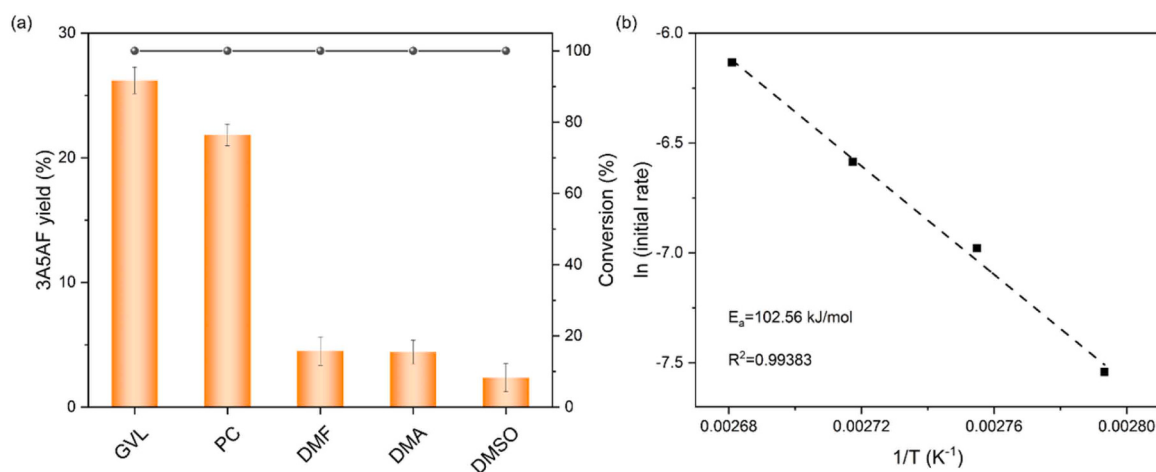


Fig. 2. (a) The effect of different solvents on the NAG conversion to 3A5AF. Reaction conditions: NAG (100 mg), NH₄SCN (200 mol%) in solvent (4 mL) at 140 °C for 30 min (b) Arrhenius plot of initial rates based on 3A5AF concentration at 85–100 °C for 30–110 min. The detailed data were shown in Fig. S4.

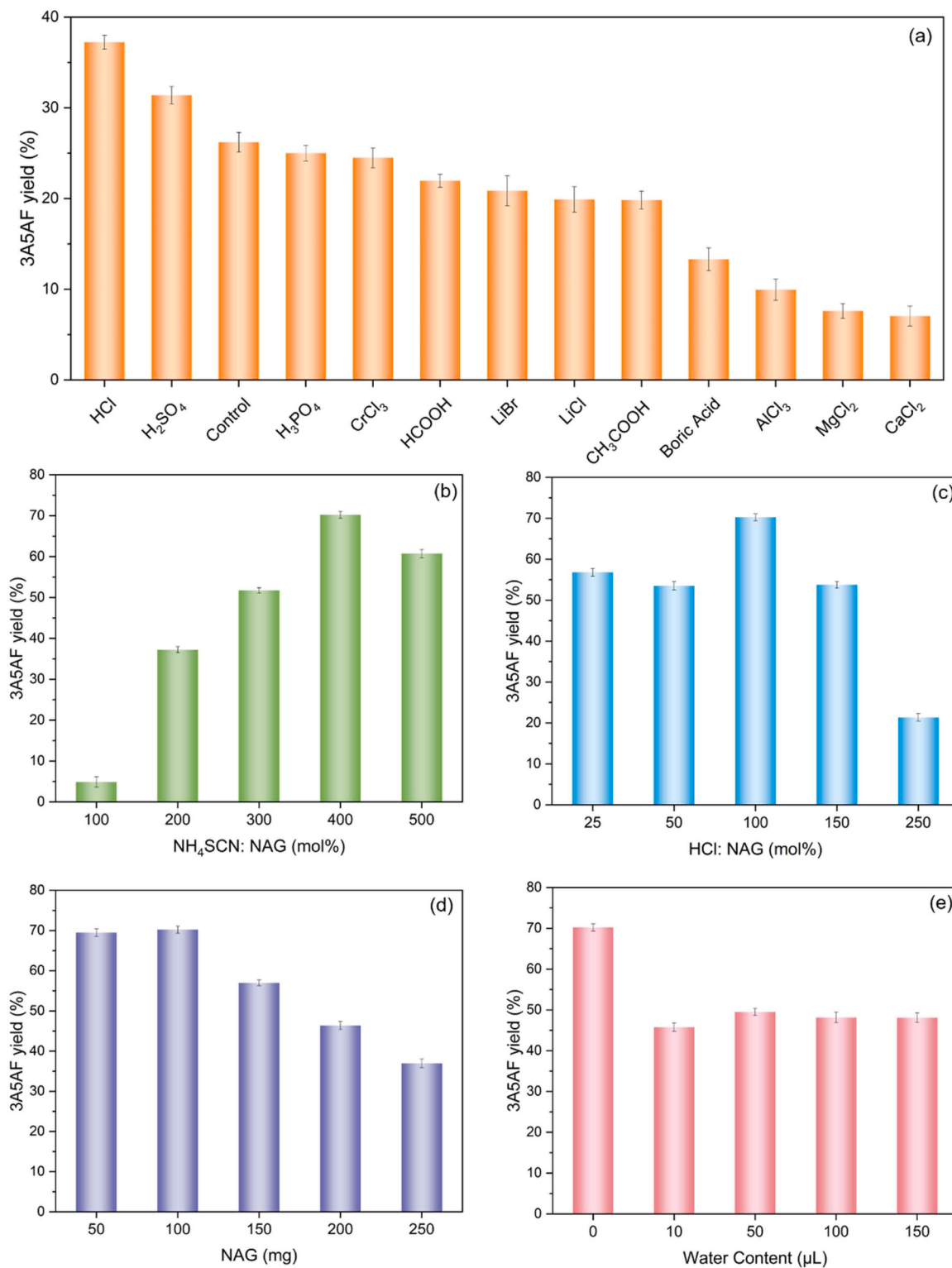


Fig. 3. (a) Additives screening on the NAG conversion to 3A5AF. Reaction conditions: NAG (100 mg), NH_4SCN (200 mol%) in GVL (4 mL) at 140°C for 30 min (b-d). Reaction optimizations of NH_4SCN dosage (b), HCl amount (c) and NAG concentration (d). Only one variable was changed in each study from the following default reaction conditions: NAG (100 mg), NH_4SCN (200 mol%) and HCl (100 mol%) in GVL (4 mL) at 140°C for 30 min (e) The effect of water on the NAG conversion to 3A5AF. Reaction conditions: NAG (100 mg), NH_4SCN (400 mol%) and HCl (100 mol%) in a total 4 mL volume of water and GVL at 140°C for 30 min.

extraction and rotary evaporation. An isolated weight yield of 40.8 wt% was achieved (equal to 54.0% molar yield), which was satisfactory considering the product loss during separation. To sum up, a green, mild and efficient method has been put forward to selectively convert NAG into 3A5AF using the biobased, nontoxic GVL solvent with the

combinational use of NH_4SCN and HCl as the promoter via the dissolution-dehydration effect.

Other sugar monomers such as glucose, fructose, xylose and glucosamine have been utilized as the substrate for the dehydration in the developed reaction system under the optimized conditions.

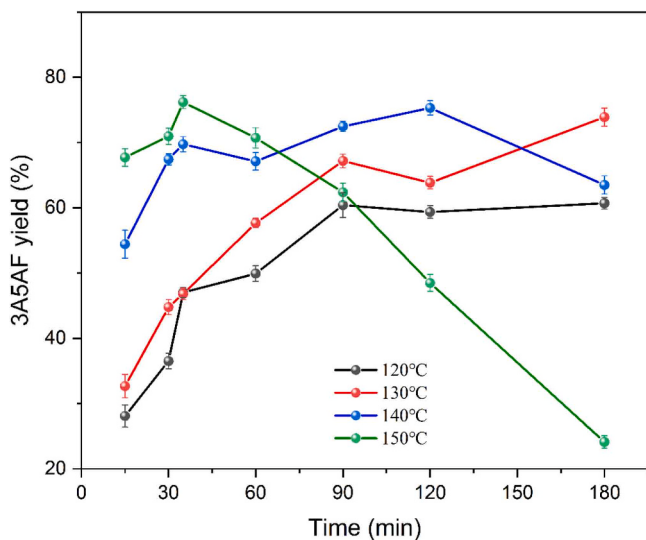


Fig. 4. Reaction optimizations of temperature and time. Reaction conditions: NAG (100 mg), NH₄SCN (400 mol%) and HCl (100 mol%) in GVL (4 mL).

However, no dehydration products such as 5-HMF, levulinic acid or furfural were observed. This infers the unique effect of the reaction system for NAG dehydration into 3A5AF.

3.4. Recyclability tests

The recyclability of the reaction system has been examined (Fig. 5). The recycling tests were first undertaken by supplying NAG and GVL (minor loss after filtration) for each run and the accumulated product yield was obtained. However, the 3A5AF yield dropped to half in the second run and to about 15% in the fourth run. An absorption treatment by using activated carbon after the reaction is quite efficient to improve the recycling ability. Extra catalyst was also supplied after the treatment because the activated carbon could partially absorb the catalyst [58]. About 60% product yield could be maintained after the fourth run, which demonstrates the satisfactory recyclability of the reaction system.

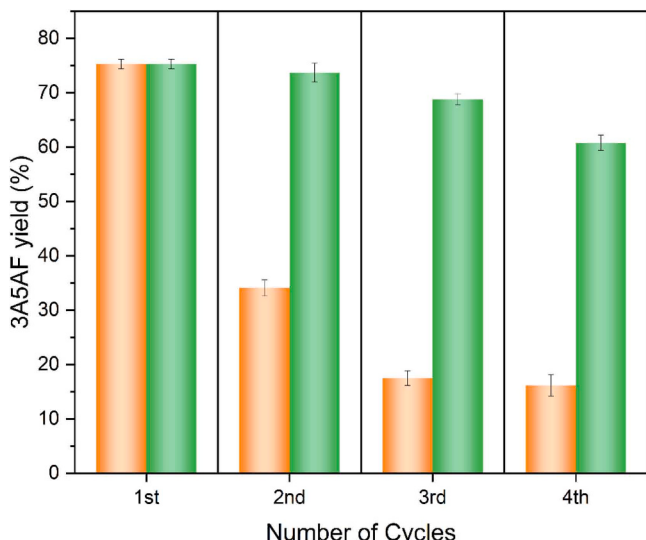


Fig. 5. The recyclability tests under the optimized conditions. Reaction conditions: NAG (100 mg), NH₄SCN (400 mol%) and HCl (100 mol%) in GVL (4 mL) at 140 °C for 2 h. The orange column and green column refer to the product yield without and with an absorption step respectively.

3.5. The elucidation on the mechanisms of the catalytic reaction

To probe the reaction intermediates, the reaction solution (at 140 °C heating for 15 min) has been subjected for the analysis on UPLC-TOF-MS (Fig. 6). The peaks located at 2.519 min and 2.955 min have been assigned to GVL and 3A5AF (the mass signals at *m/z* 101 and *m/z* 168, positive mode). The peaks ascribed to Chromogen I and Chromogen III have been identified at 0.744 min and 1.567 min (the mass signals at *m/z* 204 and 186 for M + H⁺; at *m/z* 226 and 208 for M + Na⁺). The chromogens like 3A5AF are dehydrated products from NAG but with different degree of dehydration [76,77]. The elimination of one, two and three molecules of water from NAG could lead to the subsequent formation of Chromogen I, Chromogen III and 3A5AF. The chromogens were usually regarded as the intermediates for 3A5AF formation. In addition, the NAG was directly mixed with NH₄SCN for TOF-MS analysis in water to probe the interaction between them. Nevertheless, useful information was not shown (Fig. S5). To gain further information, the ¹H and ¹³C NMR tests have been employed for the reaction solutions at 130 °C with the reaction times of 2 min, 5 min, 15 min, 30 min, 45 min and 60 min. From the ¹H NMR spectra (Fig. S6), the solvent peaks of GVL have overlapped with product signals to some extent. Without expectation, the signals of NAG was very low at merely 2 min and almost disappeared after 5 min, indicating a very rapid consumption. Meanwhile, several peaks ascribed to Chromogen III have been probed at 2 min onwards and declined after 15 min. The peaks assigned to 3A5AF started to appear after 15 min and inclined with the prolonged reaction time. The ¹³C NMR (Fig. 7) spectra were in good agreement with the ¹H NMR spectra with less signal overlapping of the solvent peaks. Based on the ¹³C NMR, the major peaks labeled by the red round dot have been ascribed to the GVL solvent. Likewise, the multiple peaks at about 40 ppm belong to the DMSO-d₆ which was added for field locking. It can be seen that the signals of NAG were readily very small (as labeled by the purple triangle) and the peaks assigned to Chromogen III was the dominant product at 2 min. Similar trends have been observed that the signals of Chromogen III steadily dropped while the peaks assigning to 3A5AF increased with the longer reaction time. The product evolution indicates that the 3A5AF was derived from the Chromogen III intermediate. Notably, in the presence of NH₄SCN catalyst, nearly complete dissolution of NAG was achieved in GVL at 130 °C and the very low peak intensity shows that the catalyst has promoted the NAG conversion in a remarkably fast manner. Hence, strong interactions between NAG and NH₄SCN was reasonably anticipated within the first few minutes. Next, the reaction solutions at lower temperatures of 90, 100 and 110 °C for 2 min have been analyzed by NMR. The NAG was partially soluble at the lower temperatures. According to the ¹H NMR spectra (Fig. S7), the signals of NAG and Chromogen I were identified for the reaction solutions at 90–110 °C for 2 min, while the peaks related to Chromogen III only appeared for the reaction solution at 110 °C. Similar results have been observed on the ¹³C NMR spectra (Fig. 8). After heating at 90 °C for 2 min, the NAG peaks could be probed on the ¹³C NMR spectrum as the major ones. The NAG mainly existed in its α -anomer form and the signals for β -anomer were relatively weak. Note that the signals for the acetamido group of NAG were not observed, it is deduced that the chemical shifts of these two carbons have altered by 2–3 ppm and then overlapped with the GVL solvent peak. This infers the possible coordination of NH₄SCN with the acetamido group on NAG to induce the changes of chemical environments. Meanwhile, the characteristic peaks ascribed to Chromogen I were observed for these solutions heating at lower temperatures, and small peaks of Chromogen III were identified when heating at 110 °C for 2 min. The NMR analyses suggested that the NH₄SCN-promoted NAG dehydration in GVL was relatively fast at elevated temperature while NAG was not soluble in GVL at room temperature. To obtain more information, DMSO-d₆ was used as the solvent instead of GVL because NAG was soluble at room temperature in the solvent and the deuterated reagent would show minimal solvent peaks to avoid signal overlaps. Three samples (including NAG,

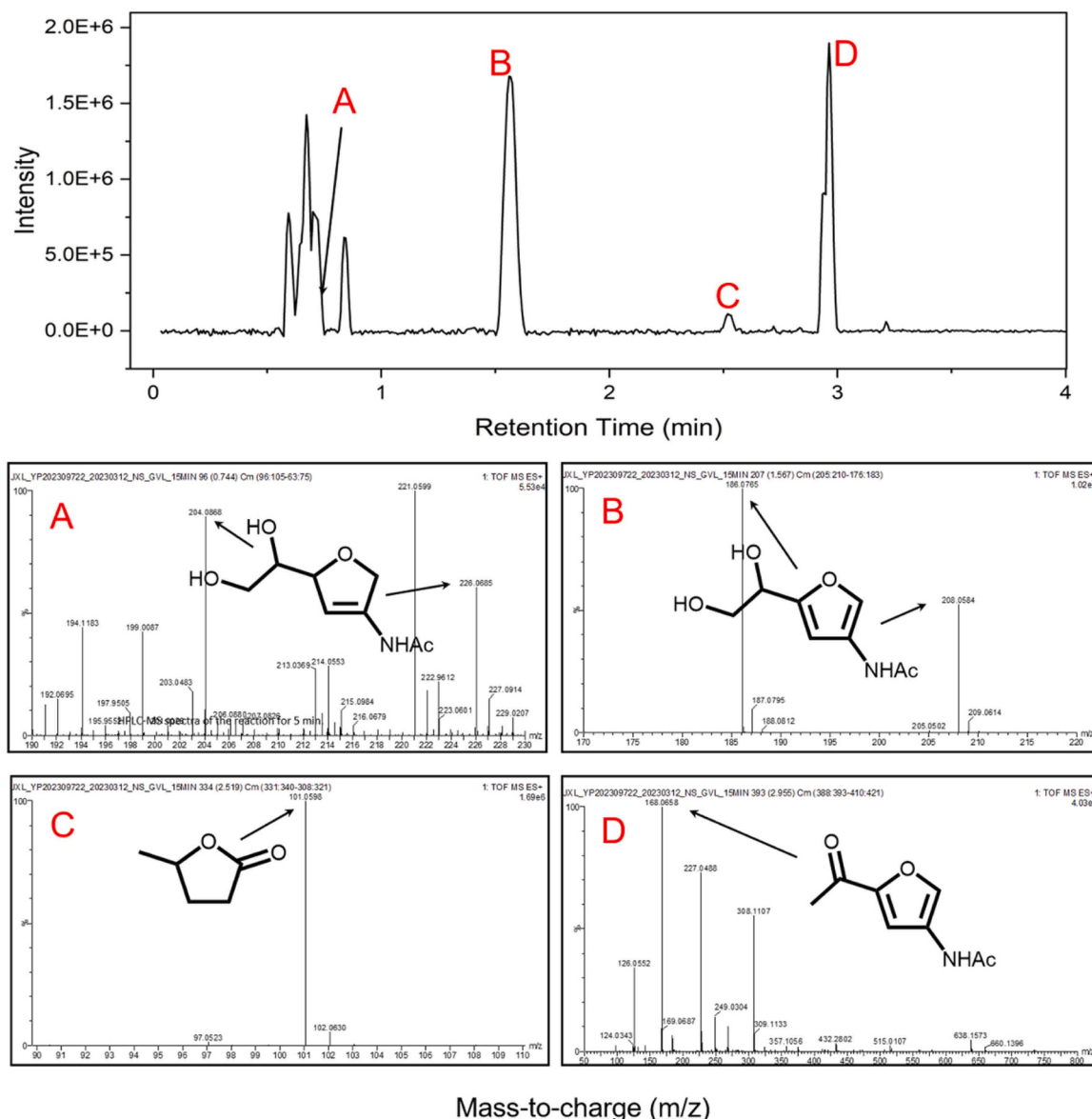


Fig. 6. UPLC-TOF-MS spectra of the reaction at 140 °C for 15 min. Reaction conditions: NAG (100 mg), NH₄SCN (200 mol%) and HCl (100 mol%) in GVL (4 mL).

NAG-NH₄SCN-RT and NAG-NH₄SCN-80) have been examined by ¹H and ¹³C NMR (Fig. S8 & S9 and Table S2 & S3). On the ¹H NMR spectra (Fig. S8), the peaks assigned to H1–3 (refer to -CH₃ in the acetamido group), H4 (refers to -NH in the acetamido group) and H7 (refers to -OH on the carbonyl carbon) have displayed slight downfield shifts in the presence of NH₄SCN. Besides, the peak broadening and downfield shifts of the H11 and H15 have been observed, which probably infers the interaction of NH₄SCN with these hydrogen atoms by forming hydrogen bonds. On the ¹³C NMR spectra (Fig. S9), an obvious downshift of the signal ascribed to the carbonyl carbon was noticed, which was consistent with the ¹H NMR and the NMR analyses in GVL that the NH₄SCN strongly interacted with the acetamido group. Based on the analyses, a plausible reaction pathway has been proposed (Scheme 1): the NAG pyranose sugar undergoes ring-opening into the straight-chain form and then shifted to furanic ring which was promoted by the interactions of NH₄SCN with the acetamido and the -OH groups. Upon the furan ring generation, the dehydration happened to eliminate one molecule of water to produce Chromogen I intermediate which further dehydrated to Chromogen III and then 3A5AF.

3.6. Preliminary studies on direct chitin conversion

The direct conversion of chitin has been undertaken in the developed reaction system (Table 1). The 3A5AF was only about 2.0% from untreated chitin under identical conditions (at 140 °C for 2 h). It is always challenging for direct chitin dehydration considering the high crystallinity and high molecular weight of chitin. Next, a series of experiments have been conducted by using ball milled (BM) chitin samples. The 3A5AF was produced with 2.2% yield at 160 °C for 60 min but not detectable under other attempted reaction conditions (with varied substrate concentration, catalyst loading, temperature and time). Hence, the crystallinity was not the determining factor that hinders 3A5AF formation. The MSHs which have been recently reported to partially dissolve native chitin [78,79] were employed as a co-solvent to facilitate dissolution of the BM chitin, nonetheless, no positive effect has been identified. In addition, a mild aging pretreatment method that established by our group [79] has been adopted to obtain 3A5AF in 3.5% yield. Lastly, the acid-impregnated chitin was ball milled into oligomers prior to reaction and an improved 3A5AF yield of about 16.0% was achieved at 140 °C for 30 min by adding 400 mol% NH₄SCN and 50 mol % HCl. Higher temperature or overdosage of the catalysts would cause

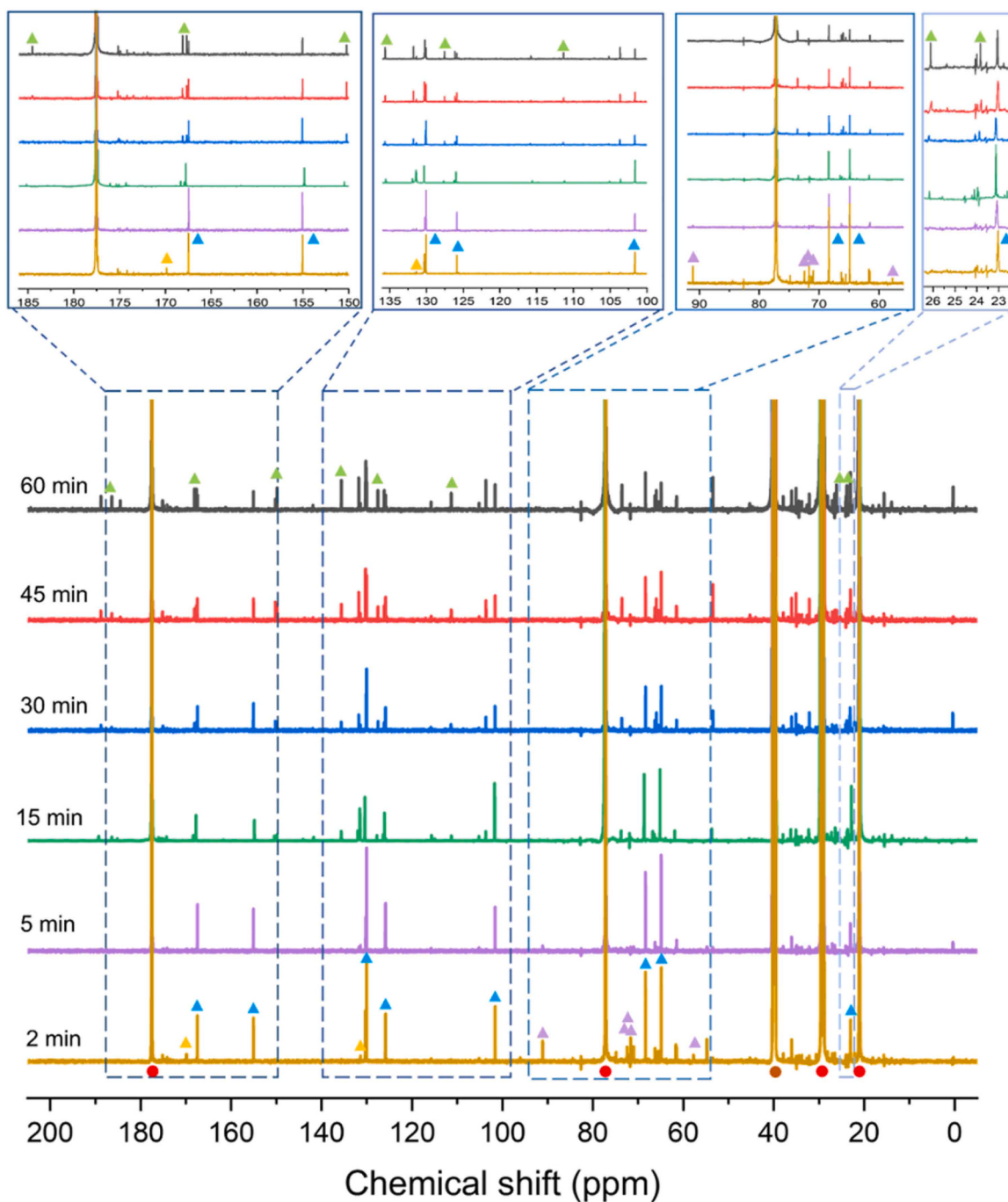


Fig. 7. ^{13}C NMR spectra of the reaction at $130\text{ }^\circ\text{C}$ for different times with TMS as reference. Reaction conditions: NAG (100 mg), NH_4SCN (400 mol%) in GVL (4 mL). Notes: ▲ NAG, ▲ Chromogen I, ▲ Chromogen III, ▲ 3A5AF, ● GVL, ● DMSO- d_6 .

the decrease in 3A5AF yield. This is in consistent with previous data that 3A5AF decomposition or side reactions were obvious at a temperature $> 140\text{ }^\circ\text{C}$ (Fig. 4). Based on the results, the major obstacle for direct chitin conversion lies in the fact that the cleavage of glycosidic bonds requires higher temperature or higher acid dosage whereas the harsher conditions would induce 3A5AF decomposition or more side reactions in the GVL system. A two-step reaction scheme to first hydrolyze chitin into the monomer and then dehydrate the NAG monomer may be a more

suitable plan for efficient 3A5AF production. Recent studies have revealed efficient hydrolysis technologies to convert chitin into the NAG monomer with high selectivity and yield. For instance, Chen et al. have utilized an affinity adsorption-enzymatic hydrolysis approach to selectively process chitin polymer into NAG under mild conditions [43]. Gözaydin et al. have employed LiBr MSHs with a very dilute acid amount to hydrolyze chitin at $120\text{ }^\circ\text{C}$ within 30 min into NAG with an outstanding yield of 71.5% [78]. Besides, Wang et al. have reported a

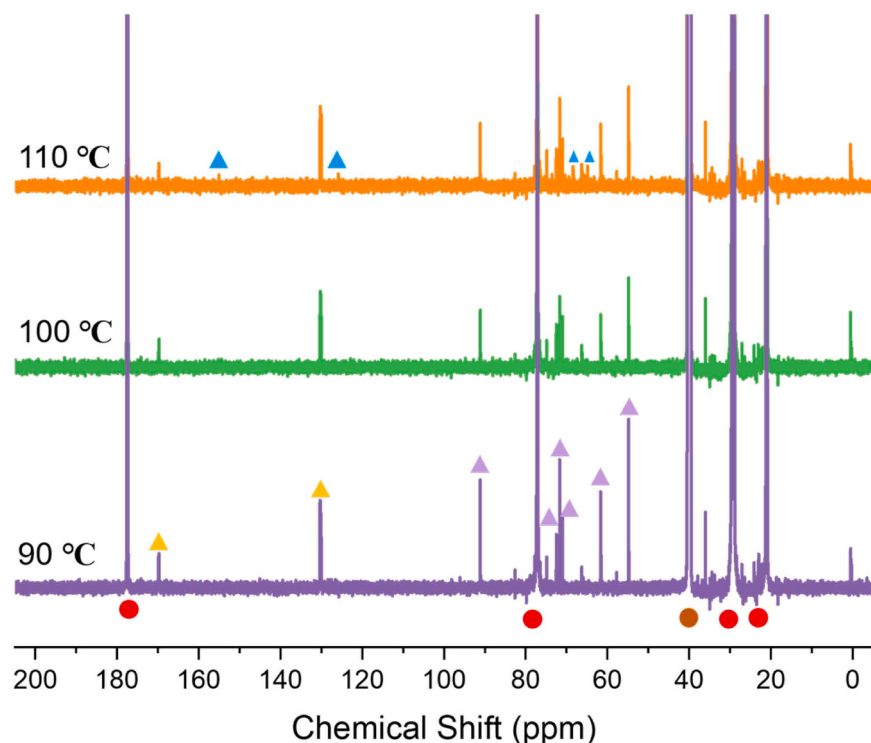
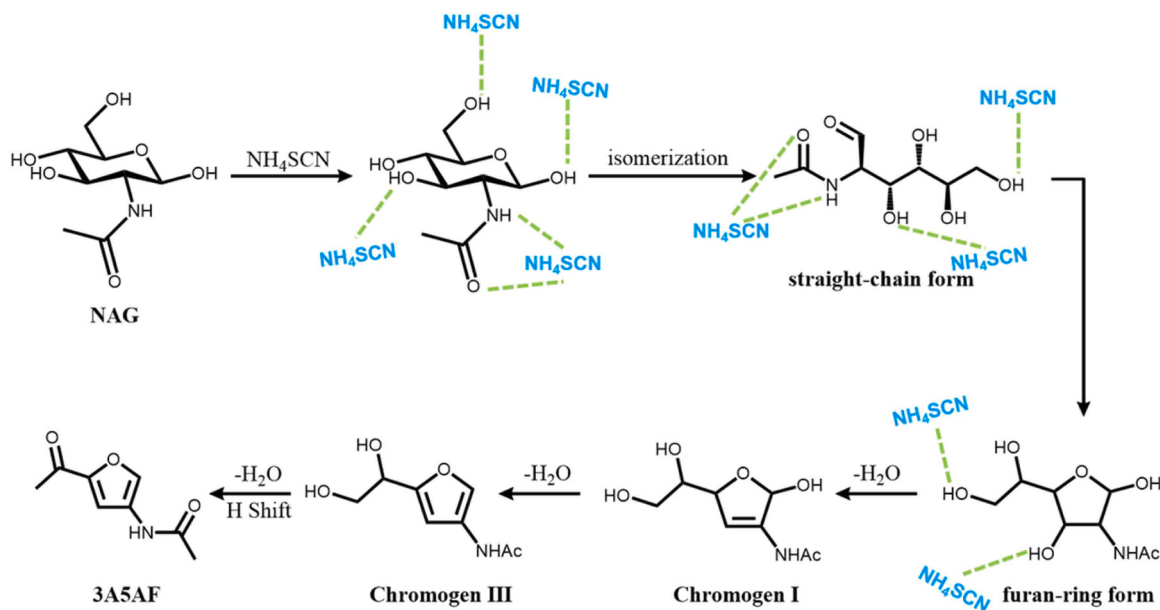


Fig. 8. ^{13}C NMR spectra of the reaction at different temperature for 2 min with TMS as reference. Reaction conditions: NAG (100 mg), NH_4SCN (400 mol%) in GVL (4 mL). Notes: \blacktriangle NAG, \blacktriangle Chromogen I, \blacktriangle Chromogen III, \bullet GVL, \bullet DMSO-d_6 .



Scheme 1. The plausible reaction pathway of NAG conversion to 3A5AF in GVL.

green and inexpensive integrated aging-hydrolysis method by using CaCl_2 MSHs with $\sim 67\%$ NAG yield [79]. The continuous progress of chitin hydrolysis technologies would enable an efficient two-step conversion scheme for 3A5AF production in the future.

4. Conclusions

In this study, the high-value furanic organonitrogen chemical 3A5AF has been obtained from the chitin-derived NAG substrate with the highest yield of 75.3% under relatively milder conditions compared to previous literatures in green biobased GVL solvent. The addition of

Table 1
Direct conversion of chitin into 3A5AF.

Entry	Substrate	Solvent ^a	NH ₄ SCN (mol%) ^b	HCl (mol%) ^b	Temp. (°C)	Time (min)	Yield (%)
1	100 mg pure chitin	GVL	200	100	140	120	2.0
2	25 mg BM chitin	GVL	600	200	160	60	2.2
3	100 mg BM chitin	GVL	400	100	140	30	0
4	25 mg BM chitin	GVL	200	200	160	60	0
5	25 mg BM chitin	GVL	400	200	160	60	0
6	25 mg BM chitin	GVL	400	400	160	60	0
7	25 mg BM chitin	GVL + 65 wt% LiBr MSH	400	200	160	60	0
8	25 mg BM chitin	GVL + 50 wt% CaCl ₂ MSH	400	200	160	60	0
9	100 mg aged chitin	GVL	400	75	180	30	3.5
10	50 mg acid-BM chitin	GVL	400	50	140	30	16.0

^a The total volume of the solvent was 4 mL, in which MSHs replaced 12.5% of GVL;

^b The amounts of NH₄SCN and HCl to be added were determined based on the moles of chitin monomer unit.

NH₄SCN was proved efficient to simultaneously promote the NAG dissolution in GVL and selectively catalyze the dehydration reaction. The combinational use of HCl together with NH₄SCN would further enhance 3A5AF yield possibly because HCl as a strong Brønsted acid could facilitate the water elimination steps. Combining the UPLC-TOF-MS and NMR studies, NH₄SCN has stimulated a very rapid consumption of NAG and promoted the NAG dehydration to Chromogen I, Chromogen III and then 3A5AF. Preliminary studies on direct chitin conversion have been investigated and the optimal 3A5AF yield was 16.0% from treated chitin sample under employed reaction conditions. The challenge in chitin conversion was identified that the hydrolysis and dehydration did not share similar optimal reaction conditions and thus the 3A5AF yield was compromised. In the regard, a two-step hydrolysis-dehydration reaction approach would be better to efficiently generate 3A5AF in high yield. The established reaction system herein has provided a more sustainable and green way to produce 3A5AF from chitin-derived biomass, contributing a new possibility in chitin-based bio-refinery for a more sustainable and green chemical industry.

CRediT authorship contribution statement

Xinlei Ji: Methodology, Investigation, Data curation, Writing - original draft. **Jia Kou:** Investigation. **Gökalp Gözaydin:** Methodology, Conceptualization. **Xi Chen:** Conceptualization, Supervision, Funding acquisition.

Declaration of Competing Interest

The authors declare the following financial interests/personal relationships which may be considered as potential competing interests: Xi Chen reports financial support was provided by Shenzhen Science and Technology Innovation Committee.

Data Availability

Data will be made available on request.

Acknowledgements

This work was financially supported by the Shenzhen Science and Technology Innovation Committee (KCXFZ20201221173413038). We acknowledge the help from the Instrumental Analysis Center of Shanghai Jiao Tong University on sample analyses.

Appendix A. Supporting information

Supplementary data associated with this article can be found in the online version at [doi:10.1016/j.apcatb.2023.123379](https://doi.org/10.1016/j.apcatb.2023.123379).

References

- Q. Hou, M. Zhen, W. Li, L. Liu, J. Liu, S. Zhang, Y. Nie, C. Bai, X. Bai, M. Ju, Efficient catalytic conversion of glucose into 5-hydroxymethylfurfural by aluminum oxide in ionic liquid, *Appl. Catal. B-Environ.* 253 (2019) 1–10, <https://doi.org/10.1016/j.apcatb.2019.04.003>.
- J. Pang, J. Sun, M. Zheng, H. Li, Y. Wang, T. Zhang, Transition metal carbide catalysts for biomass conversion: A review, *Appl. Catal. B-Environ.* 254 (2019) 510–522, <https://doi.org/10.1016/j.apcatb.2019.05.034>.
- C. Zhao, J. Yan, X. Tian, X. Xue, Y. Zhao, Progress in thermal energy storage technologies for achieving carbon neutrality, *Carbon Neutrality* 2 (2023) 2–10, <https://doi.org/10.1007/s43979-023-00050-y>.
- N.D. Miranda, J. Lizana, S.N. Sparrow, M. Zachau-Walker, P.A.G. Watson, D.C. H. Wallom, R. Khosla, M. McCulloch, Change in cooling degree days with global mean temperature increasing from 1.5 °C to 2.0 °C, *Nat. Sustain.* (2023) 1–5, <https://doi.org/10.1038/s41893-023-01155-z>.
- L. Zhang, X. Chen, Y. Chen, W. Li, K. Yang, C. Liang, Non-metal doping Ni@C as highly efficient and stable hydrodesulfurization catalysts for clean liquid fuels, *Mol. Catal.* 528 (2022), 112440, <https://doi.org/10.1016/j.mcat.2022.112440>.
- A.A.F. da Costa, L.H. d O. Pires, D.R. Padrón, A.M. Balu, G.N. d Rocha Filho, R. Luque, L.A.S. d Nascimento, Recent advances on catalytic deoxygenation of residues for bio-oil production: An overview, *Mol. Catal.* 518 (2022), 112052, <https://doi.org/10.1016/j.mcat.2021.112052>.
- K. Lee, U. Anjum, T.P. Araújo, C. Mondelli, Q. He, S. Furukawa, J. Pérez-Ramírez, S.M. Kozlov, N. Yan, Atomic Pd-promoted znrox solid solution catalyst for CO₂ hydrogenation to methanol, *Appl. Catal. B-Environ.* 304 (2022), 120994, <https://doi.org/10.1016/j.apcatb.2021.120994>.
- T. Tan, W. Wang, K. Zhang, Z. Zhan, W. Deng, Q. Zhang, Y. Wang, Upcycling plastic wastes into value-added products by heterogeneous catalysis, *ChemSusChem* 15 (2022), e202200522, <https://doi.org/10.1002/cssc.202200522>.
- Y. Zhou, J. Zhang, L. Wang, X. Cui, X. Liu, S.S. Wong, H. An, N. Yan, J. Xie, C. Yu, P. Zhang, Y. Du, S. Xi, L. Zheng, X. Cao, Y. Wu, Y. Wang, C. Wang, H. Wen, L. Chen, H. Xing, J. Wang, Self-assembled iron-containing mordenite monolith for carbon dioxide sieving, *Science* 373 (2021) 315–320, <https://doi.org/10.1126/science.aax5776>.
- K. Lee, Y. Jing, Y. Wang, N. Yan, A unified view on catalytic conversion of biomass and waste plastics, *Nat. Rev. Chem.* 6 (2022) 635–652, <https://doi.org/10.1038/s41570-022-00411-8>.
- Z. Guo, Y. Hu, S. Dong, L. Chen, L. Ma, Y. Zhou, L. Wang, J. Wang, “Spring-loaded” mechanism for chemical fixation of carbon dioxide with epoxides, *Chem. Catal.* 2 (2022) 519–530, <https://doi.org/10.1016/j.chechat.2021.12.023>.
- S. Arias, D.P. Vascoelos, D.O. Libório, J.F. Gonzalez, A.G. Câmara, C.M.B. M. Barbosa, R. Fréty, J.G.A. Pacheco, Hydrogen-free deoxygenation of industrial vegetable oil waste using Ce, Zr-NiAl catalysts for second-generation biofuels production, *Mol. Catal.* 529 (2022), 112554, <https://doi.org/10.1016/j.mcat.2022.112554>.
- B. Chen, Y. Feng, R. Huang, S. Yang, Z. Li, J. Sperry, S. Yang, X. Tang, Y. Sun, L. Lin, X. Zeng, Efficient synthesis of the liquid fuel 2,5-dimethylfuran from biomass derived 5-(chloromethyl)furfural at room temperature, *Appl. Catal. B-Environ.* 318 (2022), 121842, <https://doi.org/10.1016/j.apcatb.2022.121842>.
- Y. Lu, Z. Zhang, H. Wang, Y. Wang, Toward efficient single-atom catalysts for renewable fuels and chemicals production from biomass and CO₂, *Appl. Catal. B-Environ.* 292 (2021), 120162, <https://doi.org/10.1016/j.apcatb.2021.120162>.
- Y. Yang, S. Yuan, H. Pan, Z. Li, X. Shen, Y. Gao, Catalytically transforming cellulose into methane under natural solar irradiation, *Green. Chem.* 25 (2023) 1004–1013, <https://doi.org/10.1039/d2gc04078f>.
- W. Deng, Y. Wang, S. Zhang, K.M. Gupta, M.J. Hülsey, H. Asakura, L. Liu, Y. Han, E.M. Karp, G.T. Beckham, P.J. Dyson, J. Jiang, T. Tanaka, Y. Wang, N. Yan, Catalytic amino acid production from biomass-derived intermediates, *Proc. Natl. Acad. Sci. U. S. A.* 115 (2018) 5093–5098, <https://doi.org/10.1073/pnas.1800272115>.
- W. Deng, Y. Feng, J. Fu, H. Guo, Y. Guo, B. Han, Z. Jiang, L. Kong, C. Li, H. Liu, P.T. T. Nguyen, P. Ren, F. Wang, S. Wang, Y. Wang, Y. Wang, S.S. Wong, K. Yan, N. Yan, X. Yang, Y. Zhang, Z. Zhang, X. Zeng, H. Zhou, Catalytic conversion of lignocellulosic biomass into chemicals and fuels, *GREEN ENERGY ENVIRON* 8 (2023) 10–114, <https://doi.org/10.1016/j.gee.2022.07.003>.

[18] M.C.A. Carreira, M.C. Oliveira, A.C. Fernandes, One-pot sustainable synthesis of valuable nitrogen compounds from biomass resources, *Mol. Catal.* 518 (2022), 112094, <https://doi.org/10.1016/j.mcat.2021.112094>.

[19] X. Liu, L. Chen, H. Xu, S. Jiang, Y. Zhou, J. Wang, Straightforward synthesis of beta zeolite encapsulated Pt nanoparticles for the transformation of 5-hydroxymethyl furfural into 2, 5-furandicarboxylic acid, *Chin. J. Catal.* 42 (2021) 994–1003, [https://doi.org/10.1016/S1872-2067\(20\)63720-2](https://doi.org/10.1016/S1872-2067(20)63720-2).

[20] Q. Wang, X. Ling, T. Ye, Y. Zhou, J. Wang, Ionic mesoporous polyamides enable highly dispersed ultrafine Ru nanoparticles: A synergistic stabilization effect and remarkable efficiency in levulinic acid conversion into γ -valerolactone, *J. Mater. Chem. A* 7 (2019) 19140–19151, <https://doi.org/10.1039/C9TA02343G>.

[21] P. Guo, S. Yuan, B. Guo, S. Li, Y. Gao, Chitosan-derived carbon supported CoO combined with CdS facilitates visible light catalytic hydrogen evolution, *Catal. Sci. Technol.* 13 (2023) 1128–1139, <https://doi.org/10.1039/d2cy01962k>.

[22] N. Yan, X. Chen, Sustainability: Don't waste seafood waste, *Nature* 524 (2015) 155–157, <https://doi.org/10.1038/524155a>.

[23] G. Gözaydin, Q. Sun, M. Oh, S. Lee, M. Choi, Y. Liu, N. Yan, Chitin hydrolysis using zeolites in lithium bromide molten salt hydrate, *ACS Sustain. Chem. Eng.* 11 (2023) 2511–2519, <https://doi.org/10.1021/acssuschemeng.2c06675>.

[24] S. Xie, C. Jia, S.S. Go Ong, Z. Wang, M.-J. Zhu, Q. Wang, Y. Yang, H. Lin, A shortcut route to close nitrogen cycle: bio-based amines production via selective deoxygenation of chitin monomers over Ru/C in acidic solutions, *iScience* 23 (2020), 101096, <https://doi.org/10.1016/j.isci.2020.101096>.

[25] M. Qi, X. Chen, H. Zhong, J. Wu, F. Jin, Base-free, vanadium-catalyzed conversion of chitin into acetic acid under low oxygen pressure, *ACS Sustain. Chem. Eng.* 8 (2020) 18661–18670, <https://doi.org/10.1021/acssuschemeng.0c07147>.

[26] T.T. Pham, X. Chen, T. Söhnel, N. Yan, J. Sperry, Haber-independent, diversity-oriented synthesis of nitrogen compounds from biorenewable chitin, *Green. Chem.* 22 (2020) 1978–1984, <https://doi.org/10.1039/d0gc00208a>.

[27] J. Dai, F. Li, X. Fu, Towards shell biorefinery: Advances in chemical-catalytic conversion of chitin biomass to organonitrogen chemicals, *ChemSusChem* 13 (2020) 6498–6508, <https://doi.org/10.1002/cssc.202001955>.

[28] X. Chen, H. Yang, N. Yan, Shell biorefinery: Dream or reality? *Chem. Eur. J.* 22 (2016) 13402–13421, <https://doi.org/10.1002/chem.201602389>.

[29] X. Chen, S. Song, H. Li, G. Gözaydin, N. Yan, Expanding the boundary of biorefinery: Organonitrogen chemicals from biomass, *Acc. Chem. Res.* 54 (2021) 1711–1722, <https://doi.org/10.1021/acs.accounts.0c00842>.

[30] C. García-Sancho, I. Fúnez-Núñez, R. Moreno-Tost, J. Santamaría-González, E. Pérez-Inestrosa, J.L.G. Fierro, P. Maireles-Torres, Beneficial effects of calcium chloride on glucose dehydration to 5-hydroxymethylfurfural in the presence of alumina as catalyst, *Appl. Catal. B-Environ.* 206 (2017) 617–625, <https://doi.org/10.1016/j.apcatb.2017.01.065>.

[31] S. Song, L. Di, G. Wu, W. Dai, N. Guan, L. Li, Meso-Zr-Al-beta zeolite as a robust catalyst for cascade reactions in biomass valorization, *Appl. Catal. B-Environ.* 205 (2017) 393–403, <https://doi.org/10.1016/j.apcatb.2016.12.056>.

[32] J. Zhang, A. Das, R.S. Assary, L.A. Curtiss, E. Weitz, A combined experimental and computational study of the mechanism of fructose dehydration to 5-hydroxymethylfurfural in dimethylsulfoxide using amberlyst 70, PO_3^{2-} /niobic acid, or sulfuric acid catalysts, *Appl. Catal. B-Environ.* 181 (2016) 874–887, <https://doi.org/10.1016/j.apcatb.2014.10.056>.

[33] H. Kobayashi, T. Sagawa, A. Fukuoka, Catalytic conversion of chitin as a nitrogen-containing biomass, *Chem. Commun.* 59 (2023) 6301–6313, <https://doi.org/10.1039/d3cc00902e>.

[34] J.C. Neville, M.Y. Lau, T. Söhnel, J. Sperry, Haber-independent, asymmetric synthesis of the marine alkaloid *epi*-leptosphaerin from a chitin-derived chiral pool synthon, *Org. Biomol. Chem.* 20 (2022) 6562–6565, <https://doi.org/10.1039/d2ob01251k>.

[35] T.T. Pham, A.C. Lindsay, S.W. Kim, L. Persello, X. Chen, N. Yan, J. Sperry, Two-step preparation of diverse 3-amidofurans from chitin, *ChemistrySelect* 4 (2019) 10097–10099, <https://doi.org/10.1002/slct.201902765>.

[36] A.D. Sadiq, X. Chen, N. Yan, J. Sperry, Towards the shell biorefinery: Sustainable synthesis of the anticancer alkaloid proximicin a from chitin, *ChemSusChem* 11 (2018) 532–535, <https://doi.org/10.1002/cssc.201702356>.

[37] K.W. Omari, L. Dodot, F.M. Kerton, A simple one-pot dehydration process to convert *N*-acetyl-d-glucosamine into a nitrogen-containing compound, 3-acetamido-5-acetyl furan, *ChemSusChem* 5 (2012) 1767–1772, <https://doi.org/10.1002/cssc.201200113>.

[38] M.W. Droyer, K.W. Omari, J.N. Murphy, F.M. Kerton, Formation of a renewable amide, 3-acetamido-5-acetyl furan, via direct conversion of *N*-acetyl-d-glucosamine, *RSC Adv.* 2 (2012) 4642–4644, <https://doi.org/10.1039/C2RA20578E>.

[39] X. Chen, Y. Liu, F.M. Kerton, N. Yan, Conversion of chitin and *N*-acetyl-d-glucosamine into a N-containing furan derivative in ionic liquids, *RSC Adv.* 5 (2015) 20073–20080, <https://doi.org/10.1039/C5RA00382B>.

[40] X. Chen, S.L. Chew, F.M. Kerton, N. Yan, Direct conversion of chitin into a N-containing furan derivative, *Green. Chem.* 16 (2014) 2204–2212, <https://doi.org/10.1039/C3GC42436G>.

[41] H. Zang, J. Lou, S. Jiao, H. Li, Y. Du, J. Wang, Valorization of chitin derived *N*-acetyl-d-glucosamine into high valuable n-containing 3-acetamido-5-acetyl furan using pyridinium-based ionic liquids, *J. MOL LIQ* 330 (2021), 115667, <https://doi.org/10.1016/j.molliq.2021.115667>.

[42] J. Wang, H. Zang, S. Jiao, K. Wang, Z. Shang, H. Li, J. Lou, Efficient conversion of *N*-acetyl-d-glucosamine into nitrogen-containing compound 3-acetamido-5-acetyl furan using amino acid ionic liquid as the recyclable catalyst, *Sci. Total Environ.* 710 (2020), 136293, <https://doi.org/10.1016/j.scitotenv.2019.136293>.

[43] K. Chen, C. Wu, C. Wang, A. Zhang, F. Cao, P. Ouyang, Chemo-enzymatic protocol converts chitin into a nitrogen-containing furan derivative, 3-acetamido-5-acetyl furan, *Mol. Catal.* 516 (2021), 112001, <https://doi.org/10.1016/j.mcat.2021.112001>.

[44] D. Padovan, H. Kobayashi, A. Fukuoka, Facile preparation of 3-acetamido-5-acetyl furan from *N*-acetyl-d-glucosamine by using commercially available aluminum salts, *ChemSusChem* 13 (2020) 3594–3598, <https://doi.org/10.1002/cssc.202001068>.

[45] T. Fantoni, A. Tolomelli, W. Cabri, A translation of the twelve principles of green chemistry to guide the development of cross-coupling reactions, *Catal. Today* 397–399 (2022) 265–271, <https://doi.org/10.1016/j.cattod.2021.09.022>.

[46] M.A. Mellmer, C. Sener, J.M. Gallo, J.S. Luterbacher, D.M. Alonso, J.A. Dumesic, Solvent effects in acid-catalyzed biomass conversion reactions, *Angew. Chem. Int. Ed. Engl.* 53 (2014) 11872–11875, <https://doi.org/10.1002/anie.201408359>.

[47] F. Kerkel, M. Markiewicz, S. Stolte, E. Müller, W. Kunz, The green platform molecule gamma-valerolactone – ecotoxicity, biodegradability, solvent properties, and potential applications, *Green. Chem.* 23 (2021) 2962–2976, <https://doi.org/10.1039/d0gc04353b>.

[48] C.Y. Wong, A.W.-T. Choi, M.Y. Lui, B. Fridrich, A.K. Horváth, L.T. Mika, I. T. Horváth, Stability of gamma-valerolactone under neutral, acidic, and basic conditions, *STRUCT CHEM* 28 (2016) 423–429, <https://doi.org/10.1007/s11224-016-0887-6>.

[49] S. Dutta, I.K.M. Yu, D.C.W. Tsang, Z. Su, C. Hu, K.C.W. Wu, A.C.K. Yip, Y.S. Ok, C. S. Poon, Influence of green solvent on levulinic acid production from lignocellulosic paper waste, *Bioresour. Technol.* 298 (2020), 122544, <https://doi.org/10.1016/j.biortech.2019.122544>.

[50] A.K. Chew, T.W. Walker, Z. Shen, B. Demir, L. Witteman, J. Euclide, G.W. Huber, J. A. Dumesic, R.C. Van Lehn, Effect of mixed-solvent environments on the selectivity of acid-catalyzed dehydration reactions, *ACS Catal.* 10 (2019) 1679–1691, <https://doi.org/10.1021/acscatal.9b03460>.

[51] H. Zhang, X. Liu, J. Li, Z. Jiang, C. Hu, Performances of several solvents on the cleavage of inter- and intramolecular linkages of lignin in corncobs residue, *ChemSusChem* 11 (2018) 1494–1504, <https://doi.org/10.1002/cssc.201800309>.

[52] I.K.M. Yu, D.C.W. Tsang, A.C.K. Yip, A.J. Hunt, J. Sherwood, J. Shang, H. Song, Y. S. Ok, C.S. Poon, Propylene carbonate and γ -valerolactone as green solvents enhance Sn(iv)-catalysed hydroxymethylfurfural (HMF) production from bread waste, *Green. Chem.* 20 (2018) 2064–2074, <https://doi.org/10.1039/c8gc00358k>.

[53] M.A. Mellmer, C. Sanpitakserree, B. Demir, K. Ma, W.A. Elliott, P. Bai, R.L. Johnson, T.W. Walker, B.H. Shanks, R.M. Rioux, M. Neurock, J.A. Dumesic, Effects of chloride ions in acid-catalyzed biomass dehydration reactions in polar aprotic solvents, *Nat. Commun.* 10 (2019) 1132, <https://doi.org/10.1038/s41467-019-09090-4>.

[54] C. Sanpitakserree, A.H. Motagamwala, J.A. Dumesic, M. Neurock, Solvent and chloride ion effects on the acid-catalyzed conversion of glucose to 5-hydroxymethylfurfural, *ACS Sustain. Chem. Eng.* 10 (2022) 8275–8288, <https://doi.org/10.1021/acssuschemeng.2c00651>.

[55] Q. Lin, S. Liao, L. Li, W. Li, F. Yue, F. Peng, J. Ren, Solvent effect on xylose conversion under catalyst-free conditions: Insights from molecular dynamics simulation and experiments, *Green. Chem.* 22 (2020) 532–539, <https://doi.org/10.1039/c9gc03624e>.

[56] Y. Kim, A. Mittal, D.J. Robichaud, H.M. Pilath, B.D. Etz, P.C. St. John, D. K. Johnson, S. Kim, Prediction of hydroxymethylfurfural yield in glucose conversion through investigation of lewis acid and organic solvent effects, *ACS Catal.* 10 (2020) 14707–14721, <https://doi.org/10.1021/acscatal.0c04245>.

[57] X. Fu, Y. Hu, Y. Zhang, Y. Zhang, D. Tang, L. Zhu, C. Hu, Solvent effects on degradative condensation side reactions of fructose in its initial conversion to 5-hydroxymethylfurfural, *ChemSusChem* 13 (2020) 501–512, <https://doi.org/10.1002/cssc.201902309>.

[58] R.G. Kunz, J.F. Giannelli, Activated carbon adsorption of cyanide complexes and thiocyanate ion from petrochemical wastewaters, *Carbon* 14 (1976) 157–161, [https://doi.org/10.1016/0008-6223\(76\)90096-8](https://doi.org/10.1016/0008-6223(76)90096-8).

[59] L. Chen, Y. Xiong, H. Qin, Z. Qi, Advances of ionic liquids and deep eutectic solvents in green processes of biomass-derived 5-hydroxymethylfurfural, *ChemSusChem* 15 (2022), e202102635, <https://doi.org/10.1002/cssc.202102635>.

[60] L. Hu, Z. Wu, Y. Jiang, X. Wang, A. He, J. Song, J. Xu, S. Zhou, Y. Zhao, J. Xu, Recent advances in catalytic and autocatalytic production of biomass-derived 5-hydroxymethylfurfural, *Renew. Sust. Energ. Rev.* 134 (2020), 110317, <https://doi.org/10.1016/j.rser.2020.110317>.

[61] H. Wang, C. Zhu, D. Li, Q. Liu, J. Tan, C. Wang, C. Cai, L. Ma, Recent advances in catalytic conversion of biomass to 5-hydroxymethylfurfural and 2, 5-dimethylfuran, *Renew. Sust. Energ. Rev.* 103 (2019) 227–247, <https://doi.org/10.1016/j.rser.2018.12.010>.

[62] S. Sen, J.D. Martin, D.S. Argyropoulos, Review of cellulose non-derivatizing solvent interactions with emphasis on activity in inorganic molten salt hydrates, *ACS Sustain. Chem. Eng.* 1 (2013) 858–870, <https://doi.org/10.1021/sc400085a>.

[63] S.P.S. Chundawat, L. d. C. Sousa, S. Roy, Z. Yang, S. Gupta, R. Pal, C. Zhao, S.-H. Liu, L. Petridis, H. O'Neill, S.V. Pingali, Ammonia-salt solvent promotes cellulosic biomass deconstruction under ambient pretreatment conditions to enable rapid soluble sugar production at ultra-low enzyme loadings, *Green. Chem.* 22 (2020) 204–218, <https://doi.org/10.1039/c9gc03524a>.

[64] Q. Sun, S. Wang, B. Aguilera, X. Meng, S. Ma, F.-S. Xiao, Creating solvation environments in heterogeneous catalysts for efficient biomass conversion, *Nat. Commun.* 9 (2018) 3236, <https://doi.org/10.1038/s41467-018-05534-5>.

[65] B.A. Chambers, A.R.M.N. Afroz, S. Bae, N. Aich, L. Katz, N.B. Saleh, M.J. Kirisits, Effects of chloride and ionic strength on physical morphology, dissolution, and

bacterial toxicity of silver nanoparticles, *Environ. Sci. Technol.* 48 (2014) 761–769, <https://doi.org/10.1021/es403969x>.

[66] K. Asare-Addo, B.R. Conway, H. Larhrib, M. Levina, A.R. Rajabi-Siahboomi, J. Tetteh, J. Boateng, A. Nokhodchi, The effect of pH and ionic strength of dissolution media on in-vitro release of two model drugs of different solubilities from hpmc matrices, *Colloid Surf. B: Biointerfaces* 111 (2013) 384–391, <https://doi.org/10.1016/j.colsurfb.2013.06.034>.

[67] S.-W. Bian, I.A. Mudunkotuwa, T. Rupasinghe, V.H. Grassian, Aggregation and dissolution of 4 nm zno nanoparticles in aqueous environments: Influence of pH, ionic strength, size, and adsorption of humic acid, *Langmuir* 27 (2011) 6059–6068, <https://doi.org/10.1021/la200570n>.

[68] M. Sathish, P. Thaikaivelan, J.R. Rao, Application of gsk's model in leather making: Quantification of the environmental efficiency of a green solvent based deliming process, *ACS Sustain. Chem. Eng.* 10 (2022) 4943–4953, <https://doi.org/10.1021/acssuschemeng.1c08276>.

[69] L.D. Almeida, F.G. Delolo, A.P.S. Costa, E.V. Gusevskaya, P.A. Robles-Azocar, Catalytic aerobic epoxidation of bio-renewable alkenes using organic carbonates as green solvents, *Mol. Catal.* 527 (2022), 112400, <https://doi.org/10.1016/j.mcat.2022.112400>.

[70] H. Zang, Y. Feng, J. Lou, K. Wang, C. Wu, Z. Liu, X. Zhu, Synthesis and performance of piperidinium-based ionic liquids as catalyst for biomass conversion into 3-acetamido-5-acetylfuran, *J. MOL LIQ* 366 (2022), <https://doi.org/10.1016/j.molliq.2022.120281>.

[71] C. Wu, C. Wang, A. Zhang, K. Chen, F. Cao, P. Ouyang, Preparation of 3-acetamido-5-acetylfuran from *N*-acetylglucosamine and chitin using biobased deep eutectic solvents as catalysts, *REACT CHEM ENG* 7 (2022) 1742–1749, <https://doi.org/10.1039/d2re00118g>.

[72] Y. Du, H. Zang, Y. Feng, K. Wang, Y. Lv, Z. Liu, Efficient catalytic system for converting *N*-acetyl-d-glucosamine into valuable chemical 3-acetylaminio-5-acetyl furan, *J. Mol. Liq.* 347 (2022), 117970, <https://doi.org/10.1016/j.molliq.2021.117970>.

[73] Y. Su, G. Chang, Z. Zhang, H. Xing, B. Su, Q. Yang, Q. Ren, Y. Yang, Z. Bao, Catalytic dehydration of glucose to 5-hydroxymethylfurfural with a bifunctional metal-organic framework, *AIChE J.* 62 (2016) 4403–4417, <https://doi.org/10.1002/aic.15356>.

[74] B. Song, Y. Yu, H. Wu, Tuning glucose decomposition in hot-compressed gamma-valerolactone/water mixtures: From isomerization to dehydration reactions, *Fuel* 238 (2019) 225–231, <https://doi.org/10.1016/j.fuel.2018.10.065>.

[75] K. Wang, Y. Xiao, C. Wu, Y. Feng, Z. Liu, X. Zhu, H. Zang, Direct conversion of chitin derived *N*-acetyl-d-glucosamine into 3-acetamido-5-acetyl furan in deep eutectic solvents, *Carbohyd. Res.* 524 (2023), 108742, <https://doi.org/10.1016/j.carres.2023.108742>.

[76] M. Osada, K. Kikuta, K. Yoshida, K. Totani, M. Ogata, T. Usui, Non-catalytic synthesis of chromogen I and III from *N*-acetyl-d-glucosamine in high-temperature water, *Green. Chem.* 15 (2013) 2960–2966, <https://doi.org/10.1039/C3GC41161C>.

[77] M. Osada, S. Shoji, S. Suenaga, M. Ogata, Conversion of *N*-acetyl-d-glucosamine to nitrogen-containing chemicals in high-temperature water, *Fuel Process Technol.* 195 (2019), <https://doi.org/10.1016/j.fuproc.2019.106154>.

[78] G. Gözaydin, S. Song, N. Yan, Chitin hydrolysis in acidified molten salt hydrates, *Green. Chem.* 22 (2020) 5096–5104, <https://doi.org/10.1039/D0GC01464H>.

[79] Y. Wang, J. Kou, X. Wang, X. Chen, Acid hydrolysis of chitin in calcium chloride solutions, *Green. Chem.* 25 (2023) 2596–2607, <https://doi.org/10.1039/D2GC04246K>.